Type of the Paper (Article)

Application of New Sodium Vinyl Sulfonate –co-2-Acrylamido-2-methylpropane Sulfonic Acid Sodium Salt - Magnetite Cryogel Nanocomposites for Fast Methylene Blue Removal from Industrial Waste Water

Ayman M. Atta[1],* Sami A. Al-Hussain[2], Hamad A. Al-Lohedan[1], Abdelrahman O. Ezzat [1] and Ahmed M. Tawfeek[1]

[1] Chemistry department, college of science, King Saud University, Riyadh 11451, Saudi Arabia. (* E-mail: A.M.A, aatta@ksu.edu.sa; H.A.A., hlohedan@ksu.edu.sa; A.O.E.,ao_ezzat@yahoo.com; A.M.T., atawfik@ksu.edu.sa)

[2]Department of Chemistry, Faculty of science, Al Imam Mohammad Ibn Saud Islamic University (IMSIU), Riyadh, 13318, Saudi Arabia (sahussain@imamu.edu.sa).

* Correspondence: aatta@ksu.edu.sa; Tel.: +966-056-155-7975

Abstract: Inorganic nanoparticles based on magnetite improve the mechanical, thermal, and magnetic properties of microporous cryogel polymer composites. Here we report the synthesis of microporous cryogel based on the crosslinked sodium vinyl sulfonate (Na-VS) and 2-acrylamido-2-methylpropane sulfonic acid sodium salt (Na-AMPS). The magnetite nanoparticles were inserted into Na-VS/Na-AMPS cryogel either during its crosslinking polymerization or by *in-situ* technique after its crosslinking. The morphology, particle sizes, thermal stability and magnetite contents of Na-VS/Na-AMPS cryogel and its magnetite composites were investigated. The prepared Na-VS/Na-AMPS cryogel and its magnetite composites were used as adsorbents for methylene blue (MB) cationic dye using optimum conditions. The magnetite Na-VS/Na-AMPS cryogel composite prepared by in-situ technique achieved the best adsorption MB removal capacity for 7 cycles among the other adsorbents via chemical adsorption mechanism at room temperature.

Keywords Methylene blue; Water treatment; Magnetic nanomaterials; Cryogel; Nanocomposites.

1. Introduction

Ionic hydrophilic crosslinked polymers played important role as pH sensitive materials applied as adsorbents and drug delivery applications for the charged substances [**1-5].** The macro-porous hydrogel or cryogel is produced from the formation of ice crystals which were used as a porogen during gelation process to form pores [**6, 7**]. The polymeric cryogels attracted a particular interest among the crosslinked hydrophilic polymers due to their and their affinity to apply as sorbents for various metals to prepare nanocomposites [**6-10].** There are many factors based on the cryogelation conditions such as polymerization temperature, freezing time, freezing rate, number of thawing cycles etc. regulated the micro- and macrostructure of the cryogels [**11**]. The advanced trend to form cryogels with an internal nano-porosity in the pore walls is a complicated task [**12**]. However, the applications of cryogels were limited due to their lack of mechanical strength. Further, the

 doi:10.20944/preprints201809.0402.v1

concentration of the crosslinker affected the flexibility of the formed polymeric network chains. In this work, it is proposed that the presence of nanomaterials during the network gelation of the crosslinked cryogels may be enhance the mechanical properties and porosity of the cryogels.

The nanomaterials based on the magnetic polymer composites were widely used for water treatment due to their response to adsorb the water pollutants and to separate by an external magnet **[13-17].** The superparamagnetic properties of the iron oxides are one of the magnetic nanomaterials having sizes ranged between 50 and 180 nm. The sizes between 10 to 50 nm and below 10 nm are called small and very small superparamagnetic iron oxides nanoparticles **[18].** The sizes, distribution and shapes of iron oxides nanomaterials are based on the preparation methods based on coprecipitation, thermal decomposition, microemulsion, hydrothermal, sol-gel, flow injection, electrochemical, aerosol/vapor, and sonolysis syntheses of iron salts **[19].** The stability of iron oxides towards environmental oxidation, formation of mono and highly dispersed nanoparticles, productivity and energetically favored methods to prepare magnetic nanocomposites are targets for the researchers to increase their activity towards medical and environmental applications **[20]**. In our previous works **[21-26]**, the dispersion, stability and productivity of magnetite (Fe_3O_4) and magnetite cuprous oxides ($Fe_3O_4.Cu_2O.Fe_3O_4$) were increased in polymer composites using *in-situ* preparation technique. Moreover, their sizes distributions and magnetic properties were controlled by the *in-situ* preparation method. In the present work, sodium vinyl sulfonate (Na-VS) and 2-acrylamido-2-methylpropane sulfonic acid sodium salt (Na-AMPS) were selected as ionic monomers**,** that have strong tendency to link with iron and cupper cations to prepare their oxides into their crosslinked polymeric networks as hydrogel and cryogels **[27]**. The comparison between the abilities of the produced Na-VS/Na-AMPS networks as hydrogel and cryogel to adsorb the water pollutants is the main aim of the present work. Moreover, the determination of the optimum adsorption parameters for removal of methylene blue cationic dyes from the industrial waste water is another goal of the present work.

2. Materials and Methods

2.1. Materials

All chemicals used in this work were obtained from Aldrich Chemicals Co. The sodium vinyl sulfonate (Na-VS), 2-acrylamido-2-methylpropane sulfonic acid sodium salt (Na-AMPS) 50% used as monomers and crosslinked with N,N-methylene bisacrylamide (MBA) as crosslinker in the presence of ammonium persulfate (APS) and N,N,N′,N′-tetramethylethylenediamine (TEMED) as radical initiator, and activator for crosslinking polymerization at low temperature. The magnetite nanoparticles were prepared with high yield from reaction of anhydrous $FeCl_3$ and KI reagent after iodine removal in the presence of ammonia as reported in the previous works **[25]**. Methylene blue, produced from Sigma-Aldrich CO. is used to prepare stock solutions of 500- 2000 ppm. Buffer solution (H_3PO_4/NaH_2PO_4) was prepared by titration of 0.1 N of NaH_2PO_4 against 0.1 M HCl (for pH range 2 – 3) or against 0.1 N NaOH (for pH range 7 – 12) until the required pH is reached. The pH value was monitored using pH meter. Milli-Qdeionized water (DIW), with resistivity of 18.2MΩcm at 25 ∘C, was used to prepare the cryogels.

Preprints (www.preprints.org) | NOT PEER-REVIEWED | Posted: 20 September 2018 doi:10.20944/preprints201809.0402.v1

2.2. Preparation methods

2.2.1. Preparation of Na-VS/ Na-AMPS cryogel and its composite:

The Na-VS/Na-AMPS cryogel was prepared in the presence of MBA, APS and TEMED as crosslinked, initiator and activator, respectively. The monomers concentration in water did not exceed 20 wt% to prepare the cryogel. In this respect, Na-AMPS (2.29 g), Na-VS (2.6 g) and MBA (0.49 g) were mixed with DIW (20 mL) with stirring. APS (0.49 g) dissolved in DIW (2 mL) and TEMED (180 μL) were injected into the reaction mixture after the solution was cooled in an ice bath at 278 K. The reaction mixture was bubbled with nitrogen gas for 30 min. The reaction mixture was cooled to 253 K at a cooling rate of 275 K min^{-1} and kept constant for 24 h. The produced crosslinked Na-VS/Na-AMPS cryogel was thawed at room temperature and kept in water for 24 h to remove the unreacted monomers. The produced Na-VS/Na-AMPS cryogel white powder was filtered and dried in vacuum oven at 318K. The same procedure was used to prepare the Fe_3O_4.Na-VS/Na-AMPS cryogel nanocomposite by addition the prepared Fe_3O_4 (50 Wt % related to monomers) to the monomers solution.

2.2.2 In-situ Preparation of Na-VS/ Na-AMPS. Fe_3O_4 composite

The iron cations solution was prepared by mixing $FeCl_3.6H_2O$ (0.25 g in 20 mL distilled water) with sodium sulfite solution (1mL, of 4.8 wt% aqueous solution) at room temperature under vigorous stirring to reach equilibrium for 1 h under N_2 atmosphere. The Na-VS/Na-AMPS cryogel (1g) was immersed into iron cation solution for 24 h until it absorbed all aqueous solution. The cryogel was dried in vacuum at 303 K and the ammonium hydroxide solution (5 mL) added to swelled polymer and rinsed for 4 h. The cryogel color changed from yellow to black. The external surface of the cryogels was washed several times with water and ethanol until the filtrate became clear. The black powder washed with water and dried in vacuum over at 303 K to obtain Na-VS/Na-AMPS.Fe_3O_4.

2.3. Characterization

Fourier transform infrared (FTIR) spectrometer (Nicolet, NEXUS-670) was used to elucidate the functional groups of the cryogel and its nanocomposites with a range 4000-400 cm^{-1} using KBr pellets. The surface morphologies of Na-VS/Na-AMPS cryogel and its composites were analyzed in a Nova nano SEM 430 (FEI) environmental scanning electron microscope. The crystal size and crystal structure of the copper/iron composite was determined from XRD patterns using a BDX-3300 diffractometer with Cu Kα radiation. Thermogravimetric analysis (TGA) and stability of the nanocomposite, and cryogel was carried out using a TGA-50 SHIMADZU thermogravimetric instrument, with a TA-50 WSI thermal analyzer. Samples (5 mg) were degraded in a nitrogen atmosphere (flow rate 50 ml/min) at a heating rate of 283 K/ min.

The concentrations of MB dye in water were measured using a double beam UV−visible spectrophotometer (Shimadzu UV-1208 model at wavelength λmax equal to 662 nm).

2.4. Application of Na-VS/ Na-AMPS cryogel and its nanocomposites for water treatment

Various concentrations of MB ranged from 0.01 to 0.1 mmol L^{-1} in water were used to obtain a standard calibration curve from the relation between MB concentrations and absorbance values.A UV−visible spectrophotometer was used to determine the MB absorbance values at a wavelength of 662 nm. Concentrations of MB dye in aqueous solutions varying from 1.56 to 6.25 mmol L^{-1} (500 to 2000 mg L^{-1}) were used to determine the removal efficiencies (%) of the prepared adsorbent at optimum conditions. The adsorption kinetics of MB onto cryogel and its composites were evaluated using different concentrations of MB in 50 mL of aqueous solution in the presence of 0.02 g of the

Preprints (www.preprints.org) | NOT PEER-REVIEWED | Posted: 20 September 2018 doi:10.20944/preprints201809.0402.v1

cryogels at 298 K. The MB dye adsorption capacities at equilibrium q_e (mg.g^{-1}) and the adsorption efficiency E (%) were calculated as:

$$q_e = (C_o - C_e) \times V/m \quad (1)$$

$$E\ (\%) = (C_o - C_e) \times 100/C_o \quad (2)$$

C_o, C_e, V and m are the liquid phase concentrations of dye initially and at equilibrium (mg L^{-1}), the volume (L) of the solution and the mass of adsorbent used (g), respectively.

The MB was recovered from the polymers by collecting the polymer powder using an external magnet, pressing the gels, followed by treatment with ethanol and 0.5 mol.L^{-1} HCl and neutralization with 0.1 mol.L^{-1} NaOH aqueous solutions. The recovered gels were washed with distilled water and dried at room temperature to reuse for several adsorption experiments.

3. Results

The sulfated and sulfonated polymers have greater binding with charged cationic organic and inorganic materials due to their strong exchanges ability. In this respect, Na-VS/ Na-AMPS were selected to prepare crosslinked magnetic cryogel composites either in the presence of magnetite nanoparticles or formation of magnetite cryogel composite using *in-situ* preparation technique as represented in **Scheme 1**.

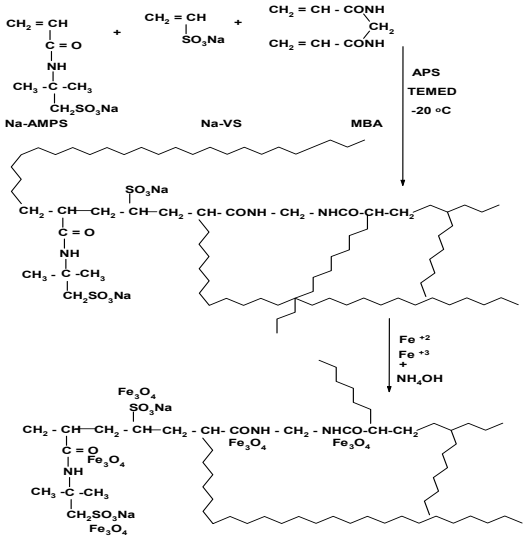

Scheme 1. Preparation of magnetite Na-VS/Na-AMPS cryogel composites.

The Na-VS/ Na-AMPS cryogel was formed through crystallization of water solvent during the crosslinking polymerization at cooling temperature 253 K as reported in the experimental section. The non-frozen liquid micro-phase based on Na-VS/ Na-AMPS among the growing contact ice crystals is polymerized using the crosslinking radical polymerization technique in the presence of MB, KPS and TEMED as crosslinker, initiator and activator, respectively. The ice crystals were used as a porogen during the crosslinking gelation process and melted after thawing to produce macro-porous networks have interconnected pores structure. The effect of magnetite nanoparticles on the morphology of Na-VS/ Na-AMPS cryogels during the cryogels networks formation is investigated.

Preprints (www.preprints.org) | NOT PEER-REVIEWED | Posted: 20 September 2018 doi:10.20944/preprints201809.0402.v1

3.1. Characterization

The chemical structures of Na-VS/ Na-AMPS and its magnetic cryogel composites (Fe_3O_4.Na-VS/ Na-AMPS and Na-VS/ Na-AMPS.Fe_3O_4 are determined from FTIR spectra represented in the Figure 1 a and b.

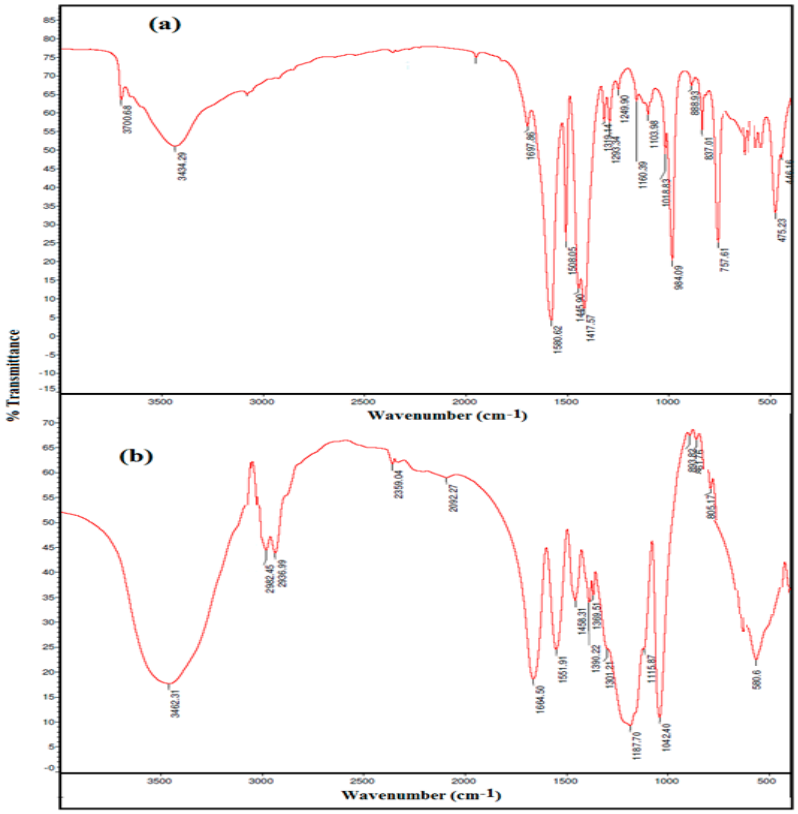

Figure 1: FTIR spectra of a) Na-VS/ Na-AMPS.Fe_3O_4 and b) Fe_3O_4.Na-VS/ Na-AMPS.

Thermogravimetric analysis (TGA) was performed under nitrogen up to 1173 K and under oxygen above 1173 K (**Figure 2**). The organic polymer segments contents are determined using nitrogen, while the oxidizing segment was used to prove whether the magnetite was still magnetite after modification or using *in-situ* polymerization technique.

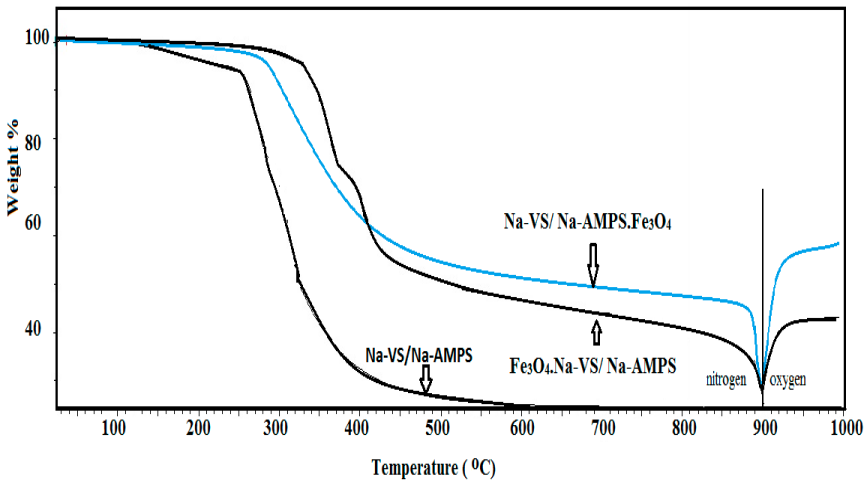

Figure 2: TGA thermograms of Na-VS/Na-AMPS cryogel and its magnetite composites.

Preprints (www.preprints.org) | NOT PEER-REVIEWED | Posted: 20 September 2018 doi:10.20944/preprints201809.0402.v1

The formation of Na-VS/Na-AMPS.Fe_3O_4 cryogel composite using *in-situ* method also elucidated from XRD difffractograms that represented in **Figure 3 a and b.**

The morphology of Na-VS/Na-AMPS cryogel, Fe_3O_4.Na-VS/ Na-AMPS and Na-VS/ Na-AMPS.Fe_3O_4 cryogel composite is investigated from SEM micrographs represented in **Figure 4a-c**.

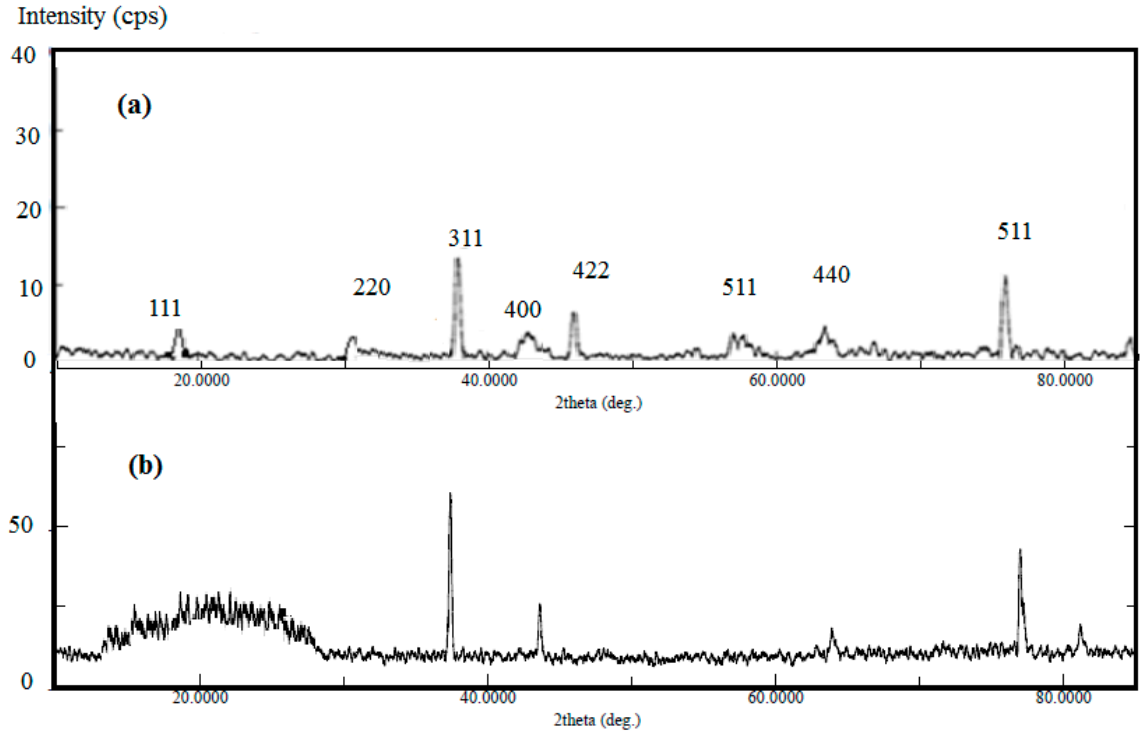

Figure 3: XRD difffractograms of a) Fe_3O_4.Na-VS/ Na-AMPS and b)Na-VS/Na-AMPS.Fe_3O_4.

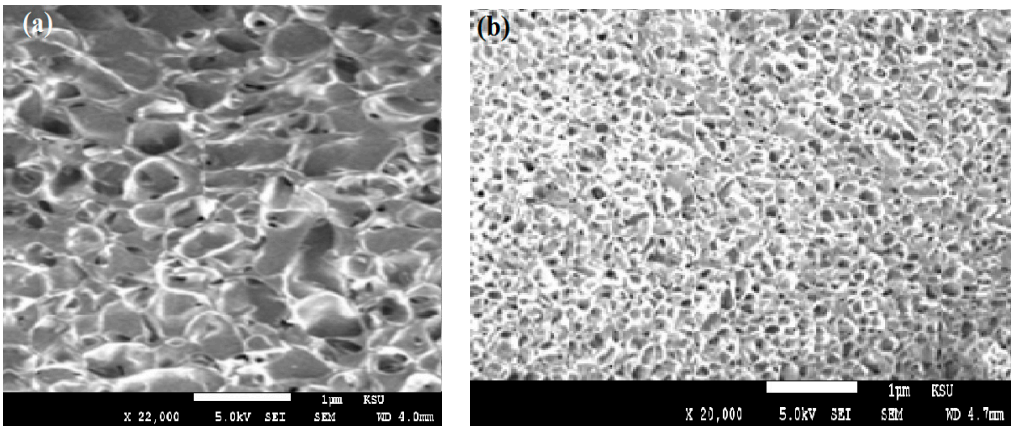

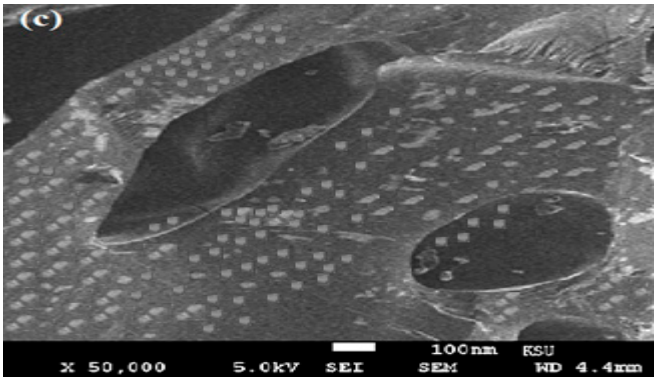

Preprints (www.preprints.org) | NOT PEER-REVIEWED | Posted: 20 September 2018 doi:10.20944/preprints201809.0402.v1

Figure 4: TEM photos of a) Na-VS/ Na-AMPS, b) Fe_3O_4.Na-VS/ Na-AMPS and c)Na-VS/ Na-AMPS. Fe_3O_4.

3.2 Magnetic Cryogel composites as MB dye adsorbents

The selection of Na-VS and Na-AMPS to prepare ionic cryogel contain sulfonate and amide group aims to use as adsorbents for charged water pollutants such as MB dye. It was noticed that the weak mechanical properties of Na-VS/ Na-AMPS cryogels due to its swelling in water affects their application as adsorbents. For these reasons Fe_3O_4.Na-VS/ Na-AMPS and Na-VS/Na-AMPS.Fe_3O_4 cryogel composites are selected to apply as adsorbents because they reduce the swelling characteristics and improved the stability of cryogel in the aqueous medium. Moreover, the magnetite is selected to inforce the Na-VS/ Na-AMPS cryogel to improve its response to collect from water by an external magnetic field as represented in **Figure 5**. In this respect, the optimum conditions to apply Fe_3O_4.Na-VS/ Na-AMPS and Na-VS/Na-AMPS.Fe_3O_4 as adsorbent such as adsorbents concentrations, aqueous solution pH, solution temperature, MB concentrations on the removal of MB from aqueous solutions are investigated in this section.

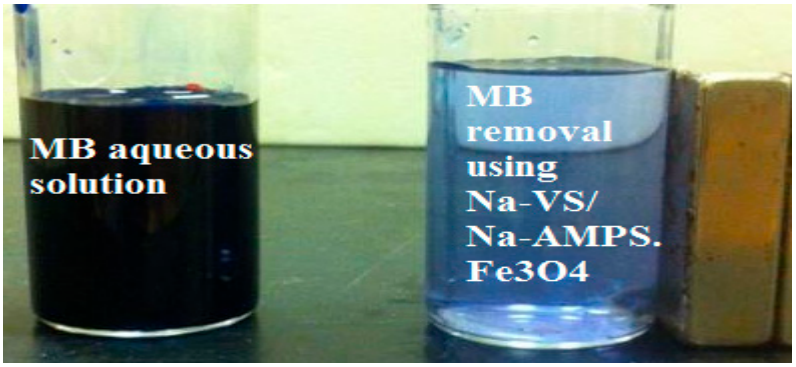

Figure 5. Photo of MB removal from water using Na-VS/ Na-AMPS. Fe_3O_4 adsorbent by external magnet.

It is very important to reduce the mass of adsorbents used to remove the pollutants from water. The relations between the mass of Na-VS/Na-AMPS, Fe_3O_4.Na-VS/ Na-AMPS and Na-VS/Na-AMPS . Fe_3O_4 cryogel composites (mg of adsorbents dispersed in 100 mL of water) and their efficiencies (E %) as adsorbents using MB dye solution (1.56 mmol.L^{-1}) under stirring for 10 minutes using a batch technique are plotted in **Figure 6** were ranged from 20 to 100 mg was added individually to 100 mL of the polluted water.

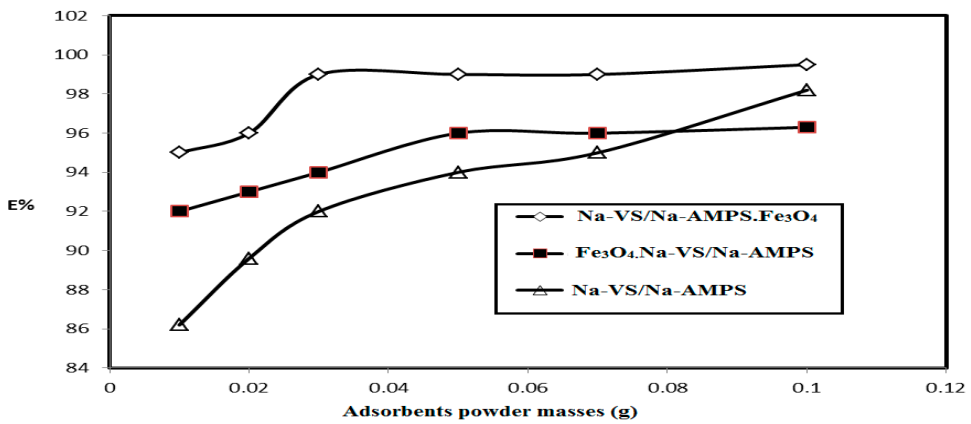

Preprints (www.preprints.org) | NOT PEER-REVIEWED | Posted: 20 September 2018 doi:10.20944/preprints201809.0402.v1

Figure 6. Effect of Na-VS/Na-AMPS cryogel and its magnetite composites contents on their MB removal efficiencies from water at room temperature.

The effect of the aqueous solution pH (2-10) on the adsorption MB removal capacities of Na-VS/Na-AMPS, Fe_3O_4.Na-VS/ Na-AMPS and Na-VS/Na-AMPS.Fe_3O_4 having 100, 50, and 30 mg adsorbent concentrations at constant ionic strength 0.01M and room temperature is illustrated in Figure 7.

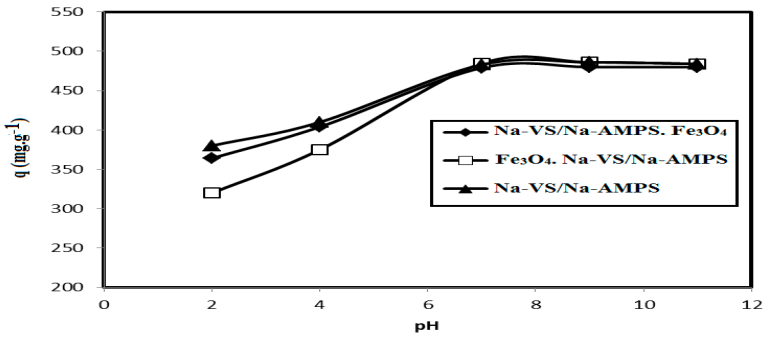

Figure 7. Effect of pH of water on the MB removal capacities of Na-VS/Na-AMPS cryogel and its magnetite composites at room temperature.

The effect of the contact times of the Na-VS/Na-AMPS, Fe_3O_4.Na-VS/ Na-AMPS and Na-VS/Na-AMPS. Fe_3O_4 adsorbents on MB removal efficiencies at their optimum concentrations and pH 7 versus their removal efficiencies MB adsorbate (500 mg. L^{-1}) is illustrated in Figure 8.

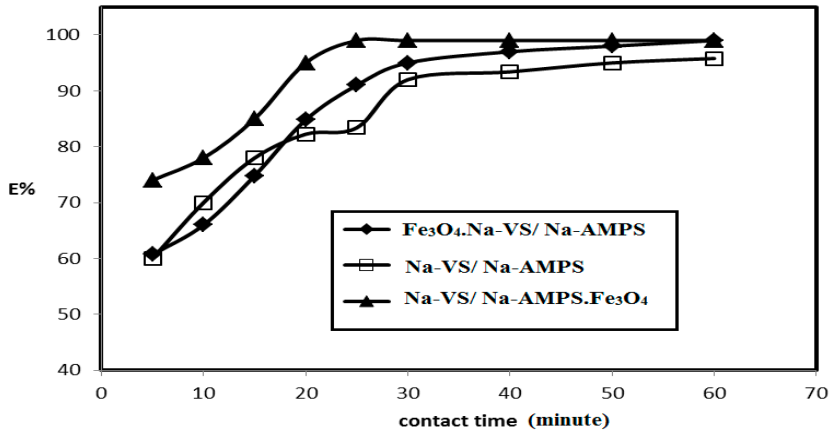

Figure 8. Effect of the contact time between Na-VS/Na-AMPS cryogels and the MB aqueous solution on their removal efficiencies at room temperature and pH 7.

The effects of MB concentrations (mmol.L^{-1}) on the removal efficiencies of the Na-VS/Na-AMPS, Fe_3O_4.Na-VS/ Na-AMPS and Na-VS/Na-AMPS.Fe_3O_4 adsorbents at their optimum conditions are represented in Figure 9.

Preprints (www.preprints.org) | NOT PEER-REVIEWED | Posted: 20 September 2018 doi:10.20944/preprints201809.0402.v1

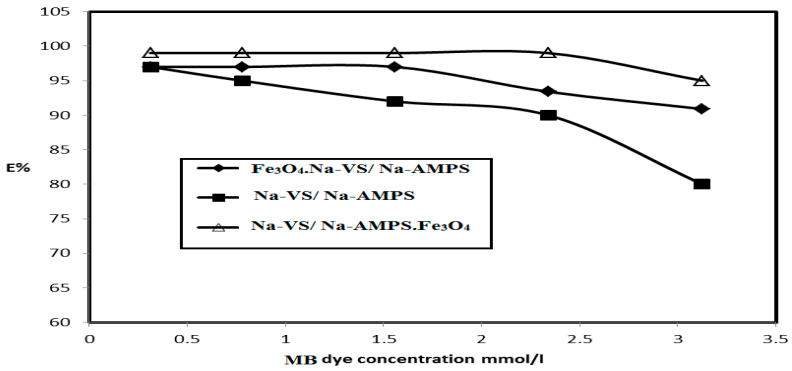

Figure 9. Effect of the MB concentrations in their aqueous solution on the removal efficiencies of Na-VS/Na-AMPS cryogels at optimum conditions.

3.3. Adsorption isotherm modeling of the MB adsorption

The chemical, physical and physico-chemical mechanisms for the adsorption of MB from aqueous solution using Na-VS/Na-AMPS, Fe_3O_4.Na-VS/ Na-AMPS and Na-VS/Na-AMPS.Fe_3O_4 adsorbents can be estimated from the adsorption isotherm models and kinetics study. The homogeneity of the adsorbent surfaces, good dispersion of the nanomaterials in the polymer composites beside the porosity of cryogel composites are the important factors to investigate the adsorption rate of adsorbate on the surfaces of the prepared adsorbents. The Langmuir and Freundlich models were selected as most famous adsorption models used to clarify the homogeneity of the adsorbate surfaces as well as the formation of MB monolayer and multilayers on the prepared adsorbent surfaces. The Langmuir and Freundlich equations are:

$$(C_e/Q_e) = [(1/Q_{max}\, K_l) + (C_e/Q_{max})] \quad (3)$$

$$\log (Q_e) = \log (K_f) + [(1/n) \times \log (C_e)] \quad (4)$$

The constants n ($g.L^{-1}$), K_l ($L.mg^{-1}$) and K_f [$(mg.g^{-1})(L.mg^{-1})^{(1/n)}$] are the empirical constant , Langmuir and Freundlich constants, respectively. The equilibrium and maximum amount of MB adsorbate are Q_e, and Q_{max} ($mg.g^{-1}$), respectively. The concentration of MB dye in the aqueous solution at equilibrium is Ce ($mg.L^{-1}$). The linear relation used to fulfill both equations 3 and 4 with highest linear coefficient (R^2) is used to explain the surface homogeneity of the adsorbent as well as the monolayer or multilayer adsorption of the MB adsorbate. In this respect, the adsorption parameters of Langmuir and Freundlich were determined and summarized in Table 1.

Table 1. Adsorption isotherm parameters of MB dye using Na-VS/Na-AMPS cryogel and its composites at temperature 298K.

Adsorbents	Langmuir isotherm parameters			Freundlich isotherm parameters			Exp. Adsorption capacity
	Q_{max} $mg.g^{-1}$	K_l $L.mg^{-1}$	R^2	n $g.L^{-1}$	K_f [$(mg.g^{-1})$ $(L.mg^{-1})^{(1/n)}$)]	R^2	Q_{max} $mg.g^{-1}$
Na-VS/Na-AMPS.Fe_3O_4	788	0.025	0.991	1.50	23.6	0.932	780
Fe_3O_4.Na-VS/Na-AMPS	748	0.075	0.987	1.04	21.8	0.929	740

Preprints (www.preprints.org) | NOT PEER-REVIEWED | Posted: 20 September 2018 doi:10.20944/preprints201809.0402.v1

Na-VS/Na-AMPS	626	0.044	0.995	1.09	33.8	0.921	660

The chemical interactions between the MB and the prepared adsorbent can be investigated from the effect of temperature on their adsorption efficiencies. In this respect, the MB solution temperatures ranged from 298 to 343 K were used to investigate the effect of temperature on the adsorption process. The thermodynamic parameters such as change in free energy (ΔG_o; KJ.mol^{-1}), change in enthalpy (ΔH_o; KJ.mol^{-1}), and changes in entropy (ΔS_o; J.mol^{-1}.K) on the adsorbent surfaces were calculated using the following equations:

$$\Delta G_o = -RT \ln (CeA/Ce) \quad (5)$$

$$\log (CeA/Ce) = \Delta S_o / 2.303R - \Delta H_o / 2.303RT \quad (6)$$

Where CeA, R and T are the adsorbent concentration (mg.L^{-1}), gas constant (8.314 J. mol^{-1}. K^{-1}) and the aqueous solution temperature (K), respectively. The (CeA /Ce) is expressed as equilibrium concentration constant (Kc) between adsorbent and MB concentrations. The calculated values of ΔG_o, ΔH_o and ΔS_o were summarized in Table 2. Moreover, the relations between ln Kc and 1/T to remove MB from their aqueous solutions using Na-VS/Na-AMPS, Fe_3O_4.Na-VS/ Na-AMPS and Na-VS/Na-AMPS . Fe_3O_4 adsorbents are represented in Figure 10.

Table 2: Adsorption thermodynamic of MB aqueous solutions using Na-VS/Na-AMPS cryogel and its composites at different temperatures.

Temp. (K)	Thermodynamic parameters								
	Fe_3O_4.Na-VS/NaAMPS			Na-VS/NaAMPS			Na-VS/NaAMPS.Fe_3O_4		
	$-\Delta G_o$ (KJ.mol^{-1})	$-\Delta H_o$ (KJ.mol^{-1})	ΔS_o (J.mol^{-1}.K)	$-\Delta G_o$ (KJ.mol^{-1})	$-\Delta H_o$ (KJ.mol^{-1})	ΔS_o (J.mol^{-1}.K)	$-\Delta G_o$ (KJ.mol^{-1})	$-\Delta H_o$ (KJ.mol^{-1})	ΔS_o (J.mol^{-1}.K)
298	21.920			24.202			31.840		
313	22.525			24.856			32.689		
318	22.726			25.074			32.972		
323	22.928			25.292			33.255		
333	23.331			25.728			33.821		
343	23.735	9.901	40.33	26.164	11.209	43.6	34.387	24.973	56.6

Preprints (www.preprints.org) | NOT PEER-REVIEWED | Posted: 20 September 2018 doi:10.20944/preprints201809.0402.v1

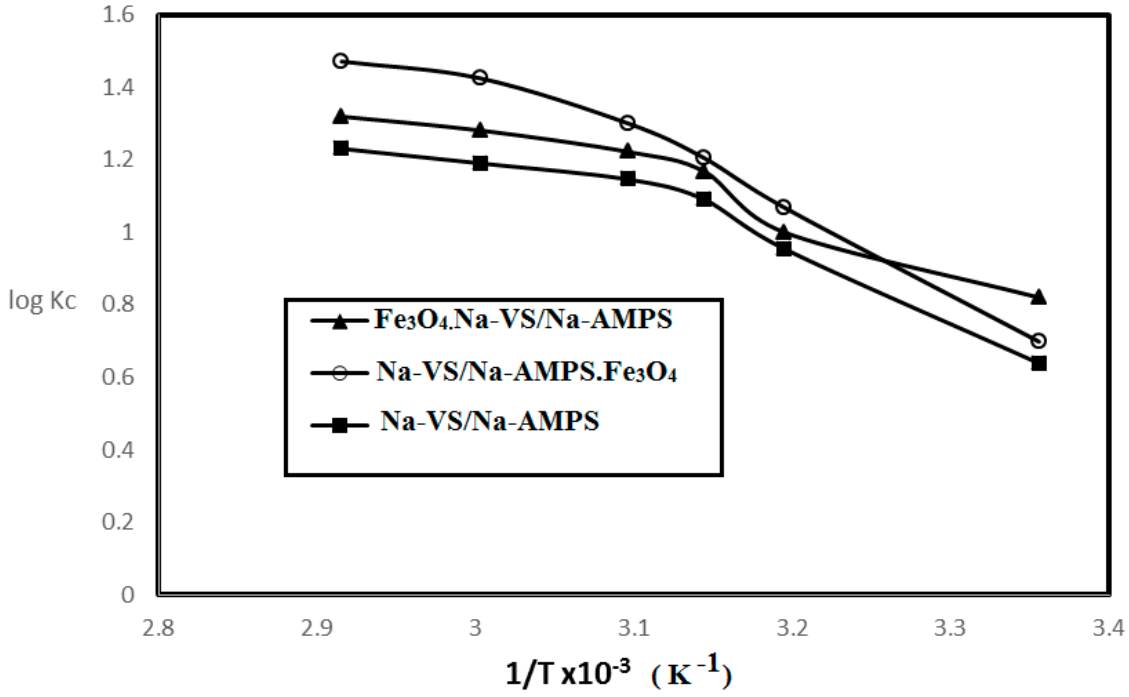

Figure 10. The relations between equilibrium concentration constant of Na-VS/Na-AMPS cryogels and the temperatures of the MB aqueous solutions using.

3.4. MB adsorption Kinetics and reuse of Na-VS/Na-AMPS cryogel composites

The adsorption rate of MB removal and rate-determining step are very important parameters used to determine the MB adsorption mechanism on the surface of cryogel and its composites. The linear relations of pseudo-first-order and pseudo-second-order kinetic models were used to analyze the MB concentrations with the contact time as expressed in the following equations:

$$\text{Log}(q_e - q_t) = [\log q_e - (k_1 t/2.303)] \quad (7)$$

$$t/q_t = [(1/k_2 q_e^2) + (t / q_e) \quad (8)$$

The adsorption capacities of MB on cryogel adsorbents q_t (mg /g) and q_e (mg /g) at time t (min) and equilibrium respectively are used to investigate the linear relations of the equations 7 and 8. The constants k_1 (min^{-1}) and k_2 (g mg^{-1} min^{-1}) are kinetic rate of MB adsorption on the surfaces cryogels using pseudo-first-order and pseudo-second-order kinetic models, respectively. The values of k_1, k_2 and their correlation coefficients (R^2) are determined and summarized in Table 3.

Table 3. Kinetic parameters of Na-VS/Na-AMPS cryogel and its composites for removal of MB from aqueous solution at temperature 298 K.

Cryogel composites	q_{exp} (mg.g^{-1})	Pseudo-first order kinetic parameters			Pseudo-second- order kinetic parameters		
		R^2	q calc. (mg.g−1)	K1 (min^{-1})	R^2	$q_{calc.}$ (mg.g^{-1})	K2 (g $mg^{-1}min^{-1}$)
Na-VS/Na-AMPS	660	0.904	261	0.033	0.997	620	0.00077

Preprints (www.preprints.org) | NOT PEER-REVIEWED | Posted: 20 September 2018 doi:10.20944/preprints201809.0402.v1

Na-VS/Na-AMPS.Fe_3O_4	780	0.912	251	0.03	0.998	740	0.06732
Fe_3O_4.Na-VS/Na-AMPS	740	0.924	251	0.03	0.997	700	0.00046

The Na-VS/Na-AMPS cryogel and its composites were reused and regenerated for several cycles to remove MB from the aqueous solution using HCl and NaOH as reported in the experimental section. The data of MB removal efficiencies (E %) of the Na-VS/Na-AMPS cryogel and its composites for 7 cycles were determined and listed in Table 4.

Table 4. Reuse Na-VS/Na-AMPS cryogel and its composites for removal of 1m,mol.L^{-1} of MB aqueous solution at 298 K.

Adsorbents	MB removal efficiency (%)		
	Na-VS/Na-AMPS	Fe_3O_4.Na-VS/Na-AMPS	Na-VS/Na-AMPS.$Fe3O_4$
Cycle 1	100	99.8	99.8
Cycle 2	5.8	99.8	99.8
Cycle 3	90.5	96.5	99.5
Cycle 4	80.2	95.4	99.4

4. Discussion

The FTIR spectra (Figure 1 a and b) elucidate the crosslinking polymerization of Na-VS and Na-AMPS monomers from the disappearance of vinyl =CH stretching, C=C stretching, and =CH out of plan bending absorption bands at 3100-3000 cm^{-1}, 1550 cm^{-1} and 900-1000 cm^{-1}, respectively. The appearance of new strong band at 3462 cm^{-1}, NH stretching of MBA and Na-AMPS amides with strong absorption in Na-VS/ Na-AMPS.Fe_3O_4 spectrum (**Figure 1b**) elucidates the formation of magnetite nanoparticles surrounded by hydroxyl groups **[28].** The interaction between magnetite and amide groups of MBA and Na-AMPS is confirmed from the formation of strong intense CONH at band 1666 cm^{-1}(Figure **1b**) which has lower intensity at 1697 cm^{-1} for Na-VS/ Na-AMPS (**Figure 1a**). Moreover, the interaction of magnetite with sulfonate groups of Na-VS/ Na-AMPS is elucidated from the S=O asymmetric stretching and symmetric S=O stretching at 1400 and 1043 cm^{-1}, respectively (**Figure 1b**). The appearance of absorption bands at 580 cm^{-1} (attributed to Fe-O bond vibration band) elucidates the presence of Fe_3O_4 nanoparticles. The TGA curves elucidate the increasing of Na-VS/ Na-AMPS thermal stability with incorporation of magnetite either during crosslinking polymerization or using *in-situ* technique. Moreover, the increasing of Na-VS/ Na-AMPS.Fe_3O_4 mass more than Fe_3O_4.Na-VS/ Na-AMPS indicates an oxidation from Fe_3O_4 to Fe_2O_3. This means that the binding of Fe_3O_4 with Na-VS/ Na-AMPS during their crosslinking polymerization more than *in-situ* technique which protects the magnetite from the oxidation. The Na-VS/ Na-AMPS.Fe_3O_4 shows two decomposition steps beginning at approximately 623 K and 773 K were detected within the nitrogen segment, resulting from the decomposition of polymer chains. The higher magnetite contents for Na-VS/ Na-AMPS.Fe_3O_4 (55 Wt %) more than Fe_3O_4.Na-VS/

 doi:10.20944/preprints201809.0402.v1

Na-AMPS (42 Wt %) confirms that the *in-situ* method is efficient to incorporate the magnetite into the Na-VS/ Na-AMPS networks.

The presence of the magnetite characteristic peaks and their crystal dimensions at 2θ = 37.53° (311), 43.53° (400), 54.51° (422), 57.27° (511), and 63.88° (440), and 77.00° (511) in the Na-VS/Na-AMPS.Fe_3O_4 diffractogram (Figure 3b) confirms the encapsulation of pure magnetite in a cubic phase (Fe_3O_4, JCPDS No. 89-3854). Moreover, the broad peaks at 2θ values ranged from 15 to 30° (**Figure 3b**) elucidates the amorphous structure of Na-VS/Na-AMPS.Fe_3O_4 cryogel polymers. The disappearance of peaks of other iron oxides **[28]** confirms the ability of Na-VS/Na-AMPS to protect the magnetite from oxidation to other iron oxides such as maghemite (γ-Fe_2O_3), hematite (α-Fe_2O_3) and the two oxyhydroxides, lepidocrocite (γ-FeOOH) and goethite (α-FeOOH). The good interaction of magnetite among cryogel matrices also elucidated from the right shifts of 2θ values of pure magnetite (Fe_3O_4, JCPDS No. 89-3854) as compared with Na-VS/Na-AMPS.Fe_3O_4 diffraction peaks (**Figure 3b**). The XRD difffractograms of magnetite and Na-VS/Na-AMPS.Fe_3O_4 cryogel (**Figure 3 a-b**) show low intense peaks which assume the small crystallite size of magnetite into Na-VS/Na-AMPS.Fe_3O_4 cryogel. The diffracting domain size (d_{xrd}) of magnetite nanoparticles encapsulated into Na-VS/Na-AMPS cryogel networks is calculated from the width of the XRD peak under the Scherrer approximation as $d_{xrd} = k\lambda/ \beta \cos \theta$; where k=0.9 is the Scherrer constant, λ=0.154nm is the X-ray wavelength, θ is the diffraction angle in degrees (2θ= 37.53°) and β is the peak width at half maximum height of the peak. The (d_{xrd}) crystallite sizes of magnetite and magnetite encapsulated into Na-VS/Na-AMPS.Fe_3O_4 cryogel are 12.32, and 8.73 nm, respectively. These data elucidates the increasing interaction between iron cations with the amide and sulfonate groups of Na-VS/Na-AMPS matrices reduces the aggregation of magnetite and reduces their sizes into Na-VS/Na-AMPS cryogel. Furthermore, the free volume in the highly crosslinked Na-VS/Na-AMPS cryogels reduces the growing of magnetite to produce ultrafine nanoparticles **[29-32]**.

The micrograph of Na-VS/Na-AMPS cryogel (**Figure 4a**) shows a spongy morphology. The formed pore walls of Na-VS/Na-AMPS (**Figure 4a**) have higher density and large pore sizes when compared with Na-VS/ Na-AMPS.Fe_3O_4 cryogel composite (**Figure 4 b**). This observation elucidates that the presence of magnetite nanomaterials during the freezing of Na-VS and Na-AMPS monomers brings about the formation of small ice crystals. Moreover, as a consequence the pore sizes of Na-VS/ Na-AMPS.Fe_3O_4 cryogel composite (**Figure 4 b**) is small with the formation of continuous channels. The presence of magnetite affects the nature of bound water into the Na-VS/ Na-AMPS hydrophilic gel **[33, 34]**. The morphology of Na-VS/ Na-AMPS.Fe_3O_4 micrograph (**Figure 4c**) elucidates that the formed magnetite into VS/ Na-AMPS networks is distributed either inside the pores or more dense among the composite pores. It was also observed that there are highly dispersed magnetite nanoparticles on the surfaces of cryogels and their pores and channels that referred to electrosteric stabilization of magnetite nanoparticles with sulfonate and amide groups of Na-VS/ Na-AMPS **[35]**.

The data (Figure 6) confirm that the optimum adsorbents concentrations for Na-VS/Na-AMPS, Fe_3O_4.Na-VS/ Na-AMPS and Na-VS/Na-AMPS . Fe_3O_4 to remove 100% of MB are 100, 50, and 30 mg, respectively. These data elucidate that the presence of magnetite either during the cryogelation (Fe_3O_4.Na-VS/ Na-AMPS) or using *in-situ* method after cryogelation (Na-VS/Na-AMPS . Fe_3O_4) improves the electrostatic interactions of polymer networks with the positive charges of MB. This

Preprints (www.preprints.org) | NOT PEER-REVIEWED | Posted: 20 September 2018 doi:10.20944/preprints201809.0402.v1

interaction increases the penetration of MB into the cryogel matrices in the presence low amount of magnetite cryogel composites. It is also noticed that the large sizes of Na-VS/Na-AMPS . Fe_3O_4 increases the adsorption of MB at the concentration of the magnetite cryogel adsorbent. It is noticed (Figure 7) that the optimum pH for MB removal adsorption capacities is pH 7. The lower MB removal adsorption capacities of the cryogel and their composites are referred to protonation of sulfonate groups Na-VS/Na-AMPS cryogel. It is noticed that the presence of magnetite into Na-VS/Na-AMPS cryogels reduces the MB removal into acidic medium more than free Na-VS/Na-AMPS cryogel without magnetite. This means that the presence of magnetite nanoparticles during the cryogelation of VS/Na-AMPS cannot protect the sulfonate groups of cryogels from protonation [**36**]. The formation of magnetite after cryogel formation protects the protonation of sulfonate anions in acidic pH and increases MB removal in acidic medium more than Fe_3O_4.Na-VS/ Na-AMPS. The stability of MB removal from their aqueous solution at pH 7 of the prepared adsorbents without improvement at pH above 7 may referred to blocking of cryogel pore sizes in alkaline medium which inhibits the cryogel MB dye uptakes [**37**]. The data (Figure 8) elucidate that the effective contact times of Na-VS/Na-AMPS, Fe_3O_4.Na-VS/ Na-AMPS and Na-VS/Na-AMPS . Fe_3O_4 adsorbents to remove MB from aqueous solution are 50, 40 and 20 minutes, respectively. These data mean that the microporous morphology of Na-VS/Na-AMPS . Fe_3O_4 adsorbents beside the good dispersion of magnetite into the Na-VS/Na-AMPS networks facilitate the diffusion and interaction of MB with the cryogel composites. The presence of magnetite into the cryogel pores forms interconnected networks that highly adsorbed high amounts of molecule adsorbate [**38**]. The data (Figure 9) elucidate that the Na-VS/Na-AMPS.Fe_3O_4 achieves high removal efficiencies (above 99.5 %) at MB concentrations up to MB 3.12 $mmol.L^{-1}$ than other adsorbents. It can be concluded that the presence of highly dispersed magnetite nanoparticles into the cryogel matrices and pores produces interconnected porous networks which facilitate the adsorption of MB dye in short time.

It is noticed that (Table 1) all Na-VS/Na-AMPS, Fe_3O_4.Na-VS/ Na-AMPS and Na-VS/Na-AMPS . Fe_3O_4 adsorbents obey the Langmuir adsorption isotherm more than Freundlich model as elucidated from their higher coefficient (R^2). These data elucidate the homogeneity of all adsorbent surfaces with the formation of monolayer MB layer onto all the prepared cryogel composites. The data (**Table 2 and Figure 10**) indicate that the Kc values increase with an increase in temperature for all the cryogel and their magnetite composites. Moreover, it is also observed that only Na-VS/Na-AMPS.Fe_3O_4 has more negative ΔH_o than -20 $KJ.mol^{-1}$ to confirm the spontaneous chemical adsorption of MB on its surfaces. The proposed mechanism for removal of MB using Na-VS/Na-AMPS and Fe_3O_4.Na-VS/ Na-AMPS is physical or physico-chemical adsorption mechanisms. This means that the in-situ technique to insert the magnetite into Na-VS/Na-AMPS facilitates both the interactions of MB with the cryogel by ion exchange with the chemical binding due to lower particle sizes of magnetite, uniform dispersion and formation of connected pores. The negative values of ΔG_o, ΔH_o (**Table 2**) elucidate the exothermic nature of the MB adsorption process using Na-VS/Na-AMPS cryogel and its composites. The negative values of ΔS_o, **Table 2**, indicate the increasing degree of freedom of the adsorbed MB dye molecules and elucidate that the increasing in the concentration of MB dye molecules in a solid-liquid interface increases the adsorption onto the cryogel surfaces. It can be concluded that the increasing of MB dye concentrations in the aqueous

solution will increase their adsorption on the cryogel surfaces in the order > Na-VS/Na-AMPS > Fe3O4.Na-VS/Na-AMPS. The Na-VS/Na-AMPS.Fe_3O_4 cryogel composite adsorbs the MB with ion exchanges mechanism and the presence of sulfonate and amide group forms complex with MB pollutant via chemical bond.

The linear and nonlinear relations of pseudo-second-order and pseudo-first-order model, respectively;[**39**] are confirmed from the low value of R^2 (Table 3) to confirm the pseudo-second-order chemical adsorption of MB on the cryogels. The agreement of the calculated values ($q_{e,cal}$, **Table 3**) and the experimental values ($q_{e,exp}$) elucidates the chemisorption of MB on the cryogels using the pseudo-second-order model **[40, 41].** The k_2 values (**Table 3**) arrange the increasing order of MB removal rate from aqueous solutions as Na-VS/Na-AMPS.Fe_3O_4 > Na-VS/Na-AMPS > Fe_3O_4.Na-VS/Na-AMPS.

The recyclability of Na-VS/Na-AMPS cryogel (Table 4) is reduced after 2 cycles to confirm its low mechanical properties. The removal efficiencies for Na-VS/Na-AMPS.Fe_3O_4 are stable for five times without significant reduction to elucidate its good mechanical and chemicals resistances. Therefore, the Na-VS/Na-AMPS.Fe_3O_4 shows higher thermal stability, porosity, faster dye removal and excellent mechanical and chemicals stability and recommended to apply as effective adsorbent to remove cationic pollutants from industrial waste water.

5. Conclusions

The incorporation of magnetite nanoparticles either during crosslinking or after polymerization of Na-VS/Na-AMPS cryogel modified its micro-porosity and mechanical properties. The *in-situ* preparation of magnetite nanoparticles among Na-VS/Na-AMPS cryogel networks produced effective, highly dispersed and low particle sizes composite more than introducing magnetite during crosslinking polymerization at lower temperature. The MB removal rate using Na-VS/Na-AMPS.Fe_3O_4 prepared by in-situ method is greater than Na-VS/Na-AMPS and Fe_3O_4.Na-VS/Na-AMPS. The Na-VS/Na-AMPS.Fe_3O_4 adsorbs the MB from their aqueous solutions with ion exchanges mechanism and via complex formation between their sulfonate and amide groups with MB pollutant.

Author Contributions: Methodology, investigation, writing—review and editing A.M. A and A.A.A.; supervision H. A. A.; revision and resources A.O.E.; methodology A. M. T.

Funding: This research was funded by Deanship of Scientific Research at King Saud University, grant number RG-235.

Acknowledgments: The authors extend their appreciation to the Deanship of Scientific Research at King Saud University for funding this work through research group No (**RG- 235).**

Conflicts of Interest: "The authors declare no conflict of interest."

References

1. Abdel-Azim, A.-A.A.; Farahat, M.S..; Atta, A.M.; Abdel-Fattah, A.A. Preparation and properties of two-component hydrogels based on 2-acrylamido-2-methylpropane sulphonic acid, *Polymers for Advanced Technologies*, 1998, 9(5), 282-289.

2. Shibayama, M.; Tanaka. T. volume phase transition and related phenomena of polymer gels. *Adv. Polym. Sci.* 1993, *1*, 109.

3. Bajpai, A. K.; Sandeep, K.S.; Bhanu S.; Kankane, S. Responsive polymers in controlled drug delivery. *Progress in Polymer Science* 2008, *33*, 1088 –1118.

4. . Atta, A.M.; Abdel-Azim, A.-A.A. Effect of Crosslinker Functionality on Swelling and Network Parameters of Copolymeric Hydrogels, *Polymers for Advanced Technologies*, 1998, 9(6), pp. 340-348.

5. Gupta, P.; Vermani. K.; Garg, S. Hydrogels: from controlled release to pH-responsive drug delivery. Drug Discovery Today, 2002, 7, 569-579.

6. Crini G.; Badot P. M.; Application of chitosan, a natural aminopolysaccharide, for dye removal from aqueous solutions by adsorption processes using batch studies: A review of recent literature. *Progress in Polymer Science*, 2008, *33*, 399-447.

7. Atta, A.M..; Arndt, K.-F., .Synthesis of charged linear and crosslinked maleic diester polymers with electron-beam irradiation, *Polymer International*, 2003, 52(3), pp. 389-398.

8. Lozinsky, V. I.; Galaev, I. Y.; Plieva, F. M.; Savinal, I. N.; Jungvid, H.; Mattiasson, B. Polymeric cryogels as promising materials of biotechnological interest. *Trends in Biotechnology* 2003, *21*, 445-451.

9. Önnby, L.; Svensson, C.; Mbundi, L.; Busquets, R.; Cundy, A.; Kirsebom, H. γ-Al_2O_3-based nanocomposite adsorbents for arsenic(V) removal: Assessing performance, toxicity and particle leakage. *Science of the Total Environment* 2014, *473–474*, 207-214.

10. Tekin, K.; Uzun, L.; Sahin, C. A.; Bektas, S.; Denizli, A. Preparation and characterization of composite cryogels containing imidazole group and use in heavy metal removal. *Reactive & Functional Polymers* 2011, *71*, 985–993.

11. Dainiak. M. B.; Kumar, A.; Plieva. F. M.; Galaev, I. Y.; Mattiasson, B. Integrated isolation of antibody fragments from microbial cell culture fluids using supermacroporous cryogels. *Journal of Chromatography* 2004, *1045*, 93–98.

12. Lozinsky, V. I. cryogels on the basis of natural and synthetic polymers: preparation, properties and application. Russian Chemical Reviews 2002, 71, 489-511.

13. Kirsebom, H.; Elowsson, L.; Berillo, D.; Cozzi, S.; Inci, I.; Piskin, E.; Galaev, I. Y.; Mattiasson, B. Enzyme-Catalyzed Crosslinking in a Partly Frozen State: A New Way to Produce Supermacroporous Protein Structures. Macromolecular Bioscience. 2013, 13, 67-76.

14. Ambasha, R. D.; Sillanpää, M. Water purification using magnetic assistance: A review. Journal of Hazardous Materials, 2010, *180*, 38-49.

15. Ozay, O.; Ekici, S.; Baran, Y.; Aktas, N.; Sahiner, N. Removal of toxic metal ions with magnetic hydrogels. *Water Research* 2009, *43*, 4403-4411.

16. Hua, M.; Zhang, S.; Pan, B.; Zhang, W.; Lv, L.; Zhang, Q. Heavy metal removal from water/wastewater by nanosized metal oxides: A review. *Journal of Hazardous Materials* 2012, *211–212*, 317-331.

17. Oliveira, L. C. A.; Rios, R. V. R. A.; Fabris, J. D.; Garge, V.; Sapag, K.; Lago, R. M. Activated carbon/iron oxide magnetic composites for the adsorption of contaminants in water. *Carbon* 2002, *40*, 2177-2183.

18. Teja, A. S.; Koh, P. Y. Synthesis, properties, and applications of magnetic iron oxide nanoparticles. *Progress in Crystal Growth and Characterization of Materials* 2009, *55*, 22-45.

19. Thorek, D. L. J.; Chen, A. K.; Czupryn, J.; Tsourk, A. Superparamagnetic Iron Oxide Nanoparticle Probes for Molecular Imaging. *Annals of Biomedical Engineering*, 2006, *34*, 23–38.

20. Kammari, R.; Das, N. G.; Das, S. K.; Nanoparticulate Systems for Therapeutic and Diagnostic Applications, Emerging Nanotechnologies for Diagnostics, Drug Delivery and Medical Devices. *Micro and Nano Technologies* 2017, 105–144.

21. Wu W, He Q, Jiang C. Magnetic Iron Oxide Nanoparticles: Synthesis and Surface Functionalization Strategies. *Nanoscale Res Lett.* 2008, *11*, 397-415.

22. Atta, A. M.; Al-Hussain, S. A.; Al-Lohedan, H. A.; Ezzat. A. O.; Tawfeek, A. M.; Al-Otabi, T. In situ preparation of magnetite/cuprous oxide/poly (AMPS/NIPAm) for removal of methylene blue from waste water. *Polymer International*. 2018, *67*, 471-480.

23. Al-Hussain, S. A.; Ezzat, A. O.; Gaffer, A. K.; Atta, A. M. Removal of organic water pollutant using magnetite nanomaterials embedded with ionic copolymers of 2-acrylamido-2-methylpropane sodium sulfonate cryogels. *Polymer International*, 2018, *67*, 166-177.

24. Atta, A. M.; Al-Hussain, S. A.; Al-Lohedan, H. A.; Ezzat, A. O.; Tawfeek, A. M.; Ahmed, M. A. In situ preparation of magnetic Fe_3O_4.Cu_2O.Fe_3O_4/cryogel nanocomposite powder via a

reduction–coprecipitation method as adsorbent for methylene blue water pollutant. *Polymer International*. 2018, https://doi.org/10.1002/pi.5582

25. Atta, A. M.; Abdel Hameed, R. S.; Al-Lohedan, H. A.; Ezzat, A. O.; Hashem, A.I. Magnetite doped cuprous oxide nanoparticles as modifier for epoxy organic coating. *Progress in Organic Coatings* 2017, *112*, 295-303.

26. Akl, Z. F.; El-Saeed, S. M.; Atta, A. M. In-situ synthesis of magnetite acrylamide amino-amidoxime nanocomposite adsorbent for highly efficient sorption of U(VI) ions. *Journal of Industrial and Engineering Chemistry* 2016, *34*, 105-116.

27. Atta, A. M.; Al-Lohedan, H. A.; Ezzat, A. O.; Eissa, Z.; Oumi, A. B. Synthesis and application of magnetite polyacrylamide amino-amidoxime nano-composites as adsorbents for water pollutants. *Journal of Polymer Research*, 2016, *23*.

28. Nguyen, T. H.; Paluck, S. J.; McGahran, A. J.; Maynard, H. D. Poly(vinyl sulfonate) Facilitates bFGF-Induced Cell Proliferation. *Biomacromolecules* 2015, *16(9)*, 2684–2692.

29. Atta, A. M.; Al-Lohedan, H. A.; Al-Hussain, S. A. Synthesis of Stabilized Myrrh-Capped Hydrocolloidal Magnetite Nanoparticles. *Molecules* 2014, *19(7)*, 11263-11278.

30. Mohan, Y. M.; Premkumar, T.; Lee, K.; Geckeler, K. E. Fabrication of Silver Nanoparticles in Hydrogel Networks. *Macromol. Rapid Commun* 2006, *27*, 1346-1354.

31. Murthy, P. S. K.; Mohan, Y. M.; Varaprasad, K.; Sreedhar, B.; Raju, K. M. First successful design of semi-IPN hydrogel–silver nanocomposites: A facile approach for antibacterial application. *J. Colloid Interface Sci.* 2008, *318*, 217-224.

32. Agnihotri, S.; Mukherji, S.; Mukherji, S. Antimicrobial chitosan–PVA hydrogel as a nanoreactor and immobilizing matrix for silver nanoparticles *Appl. Nanosci.* 2012, *2*, 179-187.

33. Kozlovskaya, V.; Kharlampieva, E.; Chang, S.; Muhlbauer, R.; Tsukruk, V. V. pH-Responsive Layered Hydrogel Microcapsules as Gold Nanoreactors. *Chem. Mater* 2009, *21*, 2158- 1267.

34. Okoroafor, E. U.; Newborough, M.; Highgate, D.; Augood, P. Effects of thermal cycling on the crystallization characteristics of water within crosslinked hydro-active polymeric structures. *J Phys D Appl Phys* 1998, *31*, 3130-3138.

 doi:10.20944/preprints201809.0402.v1

35. Patil, R. D.; Mark, J. E.; Apostolov, A.; Vassileva, E.; Fakirov, S. Crystallization of water in some crosslinked gelatins. *Eur Polym J.* 2000, *36*, 1055-1061.

36. Liang, Y. N.; Hu, J.; Tam, M. K. C.; Hu, X.; CuO_x nanotubes *via* an unusual complexation induced block-like self-assembly of poly(acrylic acid). *RSC Adv.* 2012, *2*, 9531-9537.

37. Nart, Z.; Apohan, N. K. Preparation, characterization and drug release behavior of poly (acrylic acid–co-2-hydroxyethyl methacrylate-co-2-acrylamido-2-methyl-1-propanesulfonic acid) microgels. *J. Polym. Res.* 2011, *18*, 869-874.

38. Ng, L.T.; Ng, K. S. Photo-cured pH-responsive polyampholyte -coated membranes for controlled release of drugs with different molecular weights and charges. *Radiat. Phys. Chem.* 2008, *77*, 192 -199.

39. Sahiner, N.; Sagbas, S. Sucrose based ionic liquid colloidal microgels in separation of biomacromolecules. *Separation and Purification Technol* 2017, *196*, 191-199

40- Ho, Y. S.; McKay, G. Pseudo-second order model for sorption processes. *Process Biochem*. 1999, *34*, 451–465.

41- Zhu, H.; Fu, Y.; Jiang, R.; Yao, J.;, Liu, L.; Chen, Y.; Xiao, L.; Zeng, G. Preparation, characterization and adsorption properties of chitosan modified magnetic graphitized multi-walled carbon nanotubes for highly effective removal of a carcinogenic dye from aqueous solution. *Appl. Surf. Sci.* 2013, *285*, 865-873.